Vertical and horizontal distribution of wind speed and air temperature in a dense vegetation canopy

Jacobs, A.F.G.; van Boxel, J.H.; El-Kilani, R.M.M.

Published in:
Journal of Hydrology

DOI:
10.1016/0022-1694(94)05093-D

ELSEVIER

Journal of Hydrology 166 (1995) 313–326

Journal of Hydrology

[3]

Vertical and horizontal distribution of wind speed and air temperature in a dense vegetation canopy

A.F.G. Jacobs[a,*], J.H. van Boxel[b], R.M.M. El-Kilani[a]

[a]*Department of Meteorology, Agricultural University, P.O. Box 9101, NL-6700 HB Wageningen, Netherlands*

[b]*Department of Physical Geography and Soil Science, University of Amsterdam, Nieuwe Prinsengracht 130, NL-1018 VZ Amsterdam, Netherlands*

Received 6 May 1993; accepted 5 April 1994

Abstract

Wind speed and temperature were measured within a corn row canopy to investigate horizontal and vertical variability of the mean wind speed and temperature. It appears that the mean wind speed can vary between 20% and 30% from its horizontal mean value. In the narrow row crop, the horizontal mean air temperature varies between 0.1°C (night-time) and 0.35°C (daytime) from the spatial mean value. Exceptions occur around noon in daytime when direct irradiation dominates and where the direct beam illuminates the within-row space of the canopy. Then, deviations of 1°C or more from the horizontal mean value are observed. Attention was focused on finding adequate scaling parameters of the within-canopy wind speed and air temperature profiles under various atmospheric stratification states. During daytime and night-time, the above-canopy friction velocity appears to be a good scaling parameter. Clear nights, however, are exceptions, when the above-crop wind speed drops to a very low value. Then, the within-canopy free convection velocity scale appears to be an appropriate scaling parameter for within-canopy processes. During daytime, the within-canopy temperature profiles scale well with the above-canopy temperature scale, T^*, for stationary irradiation and wind speed regimes. On calm nights, however, the relative within-canopy temperature profile scales very well with the within-canopy free convection temperature scale, Θ^*.

1. Introduction

Air movement as well as the air temperature just above and within a row crop canopy is characterized by complex interactions of the air mass above and within the

* Corresponding author.

SSDI 0022-1694(94)05093-D

canopy. The air flow far above a horizontally homogeneous canopy behaves two-dimensionally. In the vicinity of the top of the canopy, in the so-called roughness layer, the flow becomes more complex, instantaneously as well as on average. Large deviations from the spatially averaged mean value can occur owing to direct sensing of individual roughness elements by the flow. Here, the mean flow becomes essentially three-dimensional and spatially variable. As a rule of thumb, the vegetation layer lies between $0 < z < (d + z_0)$ and the roughness layer between $(d + z_0) < z < (d + 20z_0)$, where d is the displacement height and z_0 is the roughness length (Tennekes, 1982). Within the canopy, between the roughness elements, this three-dimensional behaviour will be enhanced, as there the flow is completely disturbed by elements of the canopy.

The extensive literature on the temperature behaviour just above and within crop canopies is understandable, as this temperature distribution is directly connected to the transport of heat and water vapour. However, there is a lack of experimental wind speed profile evidence, which is properly averaged spatially, because velocity is a vector quantity, which is much more difficult to measure accurately than a scalar quantity. A special problem just above and within canopy crops is that, close to the elements of the crop canopy, the flow field and other surface processes are influenced by individual surface elements. This means that, even for a so-called homogeneous surface, horizontal inhomogeneities will emerge automatically when attention is focused close to the surface elements.

Until now, only in a small number of outdoor experiments close to the surface elements have aspects of the vertical and horizontal variability of the flow characteristics been measured. For example, Shaw et al. (1974) and Mulhearn and Finnigan (1978) observed turbulence and turbulent transport of momentum and heat above a rough surface rather close to the roughness elements. Stigter et al. (1976) studied the horizontal homogeneity of the temperature and moisture within a maize canopy. Graser et al. (1987) studied temperature patterns within sorghum canopies with different row spacing.

It is intended to delineate some of the characteristics of canopy flows. In particular, the objectives are (1) to obtain insight into the horizontally averaged wind speed and air temperature profiles and their variabilities and (2) to examine the governing scaling parameters of the within-canopy wind speed and air temperature profiles.

2. Theory

Under a steady state and a thermally stratified atmosphere, the wind speed profile and the temperature profile near the Earth's surface in the surface layer ($z > d + 20z_0$) can be described adequately by the profiles (Arya, 1988)

$$u(z) = (u^*/\kappa)\{\ln[(z-d)/z_0] - \psi_m[(z-d)/L]\} \tag{1}$$

and

$$T(z) - T(d+z_0) = (T^*/\kappa)\{\ln[(z-d)/z_0] - \psi_h[(z-d)/L]\} \tag{2}$$

where $u(z)$ and $T(z)$ are the mean wind speed and mean air temperature, respectively, at height z, d is displacement height, z_0 is roughness length, u^* is the friction velocity, T^* is the scaling temperature defined by $T^* = -\overline{w'T'}/u^*$, $\kappa = 0.4$ is Von Kármán's constant, L is Obukhov's stability length scale, and ψ_m and ψ_h are stratification correction functions for momentum and heat, respectively.

During daytime, the within-canopy processes are dominated by the large eddy exchange mechanism (Finnigan and Raupach, 1987; Jacobs et al., 1992). Under these conditions, an appropriate within-canopy scaling velocity and scaling temperature may equal the above-canopy friction velocity, u^*, and scaling temperature, T^*, respectively. During night-time with strong wind conditions, the exchange mechanism may be dominated by the above-canopy flow regime, and the velocity and temperature regime may scale also with u^* and T^*, respectively.

At night under low wind speed conditions, however, a decoupling between the above- and within-canopy processes develops. Then, within the canopy, a free convection state occurs in which free convection cells are generated by the relatively warm canopy floor (Jacobs et al., 1992). By radiative cooling, the air at the upper part of the vegetation is stabilized and thus the unstable lower vegetation layer is capped and thereby decoupled from the above-canopy region. Then, the crop height and the buoyancy flux from the soil surface are the two variables important to this free convection state. Combining these scales yields a free convective velocity scale, w^*, and a free convective temperature scale, Θ^* (Tennekes and Lumley, 1972):

$$w^* = [(hg/T)(\overline{w'T'})_0]^{1/3} \tag{3}$$

and

$$\Theta^* = -(\overline{w'T'})_0/w^* \tag{4}$$

where g is gravity, h is canopy height and $(\overline{w'T'})_0$ is the kinematic heat flux at the soil surface. An appropriate estimate at night-time for the kinematic heat flux at the soil surface is $(\overline{w'T'})_0 \approx q_s/(\rho c_p)$, where q_s is the soil heat flux at the ground and (ρc_p) is the volumetric heat capacity of air, because during night-time most of the soil heat flux at the base of a reasonably dense canopy is transformed into sensible heat (Garratt and Segal, 1988).

3. Measurement site and instrumentation

In addition to a continuous programme of measurements of fluxes of heat, mass and momentum above and within a maize crop canopy (Jacobs and Van Boxel, 1988a), a more detailed turbulence and within-canopy experiment was carried out at the experimental farm at Sinderhoeve (51°59′N, 5°45′E) during 2 weeks in July 1986. Only instruments relevant to this study will be discussed here.

Above the crop, the mean wind profile was measured with cup anemometers at 11 heights above the ground (1.7, 2.2, 2.85, 3.5, 4.25, 5.0, 6.0, 7.0, 8.0, 9.0 and 10 m). The cup-type anemometers had a starting speed of 0.20 m s^{-1} and a first-order response distance (66%) of 0.90 m. The above-canopy wind profiles were used to calculate the

two surface characteristics, d and z_0, and their course during the growing season (Jacobs and Van Boxel, 1988a,b). The mean temperature and moisture were measured at heights of 2.0 and 4.0 m with aspirated psychrometers. At a height of 4.5 m, a 3-D sonic anemometer (Kaijo Denki, Tokyo, model DAT-310), an additional fast-response thermometer and a Lyman-α humidiometer were installed. These instruments provide data about the above-crop thermal stratification of the atmosphere.

Within the canopy, at $0.25D$ between the rows, where D is the row distance, the mean wind speed profile was measured with hot-sphere anemometers (Stigter et al., 1976) at heights of 0.1, 0.2, 0.3, 0.4, 0.7, 1.0 and 1.4 m. To gain insight into the horizontal variability of the wind speed, at levels of 0.3 and 0.7 m, measurements were made at $0.25D$, $0.50D$, $0.75D$ and $1.00D$. Moreover, at $0.25D$ between two rows, the mean temperature profile was measured with fast-response thermometers (Van Asselt et al., 1991) at heights of 0.0, 0.1, 0.2, 0.3, 0.5, 0.7, 1.0 and 1.4 m. The measurement accuracy of the mean temperature was better than 0.05°C, and the first-order time constant of the thermometers was about 0.08 s. To gain also insight into the horizontal variability of the temperature, at two levels (0.3 and 0.7 m), measurements were made at $0.25D$, $0.50D$, $0.75D$ and $1.00D$.

The hot-sphere anemometers are very suitable for measuring low wind speeds (measuring range 0.02–2.0 m s^{-1}). As these anemometers have no moving parts, they cannot be blocked by flapping leaves or other canopy structures. The hot-sphere anemometers were calibrated in a low-wind-speed tunnel, to an accuracy of better than 5%. A restriction of hot-sphere anemometers is that the absolute wind speed is measured and no information is obtained about the wind direction. Their measuring volume is small (sphere diameter approximately 3 mm), and their first-order response time is wind speed dependent and is about 2 s at 1 m s^{-1}, which is relatively long. In addition, a 1-D sonic anemometer (Kaijo Denki, model PAT-110) plus an additional fast-response thermometer and a Lyman-α humidiometer were installed at a height of 0.7 m inside the canopy in the middle of the row, to measure the within-canopy transport of heat and water vapour.

The maize crop (*Zea mays* L., cv. 'Vivia') was planted in rows 0.75 m apart with plants 0.11 m apart in the row. The rows were orientated NNE–SSW. During the detailed turbulence experiment, the crop was at the end of the vegetative state, and had a height, h, of 1.70 m and a one-sided plant area index, PAI, of 3.6. The PAI is the sum of the leaf area index, LAI, and the stem area index, SAI. The plant area distribution, a, which is an important parameter in modelling the within-canopy flow, has been plotted in Fig. 1 in schematic and nondimensional form. The plant area distribution is defined as the one-sided plant area (i.e. leaves and stems) per unit volume of air. The plant characteristics were estimated using the leaf tracing method suggested by Kvet and Marshall (1971). The fetch was dependent on the wind direction and ranged between 200 and 800 m.

The fast-response thermometers were sampled at 5 Hz. All other fast-response instruments were sampled at 10 Hz, whereas all slow-response instruments were sampled at 1 Hz. The signals were carried to a mobile measurement van, about 100 m from the instruments. Here, the raw data were stored on a digital magnetic tape for

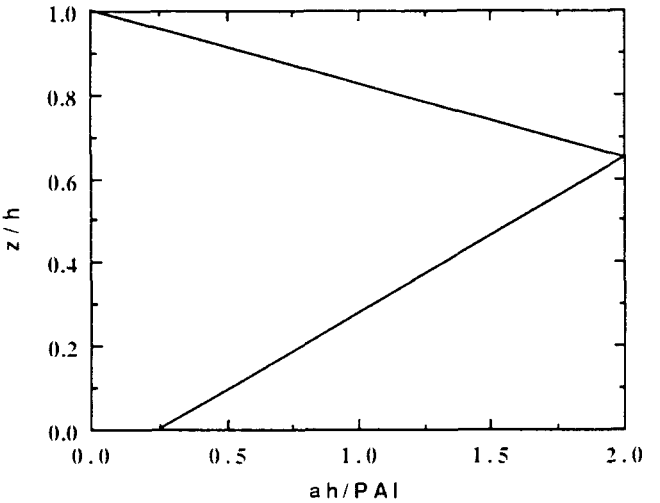

Fig. 1. The plant area distribution, a, i.e. one-sided plant area per volume air ($m^2\ m^{-3}$) nondimensionalized with the canopy height, h, and scaled with the plant area index PAI vs. the nondimensional height, z/h. The area under the curve is equal to unity with regard to the y-axis.

later analysis. Further details on measurement techniques have been provided elsewhere (Jacobs and Van Boxel, 1988a).

4. Vertical within-canopy wind speed and temperature profiles

Two days with different weather regimes have been selected for a detailed analysis. The most important weather conditions have been portrayed in Fig. 2; 29 July was a windy day with intermittent cloudiness, whereas 30 July was a moderatly fine day with less wind and a more regular irradiation pattern.

In Fig. 3, the hatched area shows the range of the 30 min means of the wind speed. These profiles were measured on two days (29 July and 30 July 1986) near the centre of the canopy row at $0.25D$. The heights have been nondimensionalized with the height of the canopy ($h = 1.70$ m), and the wind speeds have been nondimensionalized with the friction velocity, u^*.

The left-hand part of Fig. 3 shows data selected for near-neutral stratification ($|L| > 30$ m, where L is the Obukhov length for above the canopy). It can be inferred that the maximal wind speed occurs at the top of the canopy. A second local maximum occurs in the lower region of the canopy ($z/h \approx 0.1$).

It can be concluded that the dimensionless profiles are similar in shape under near-neutral stratification and scale with the above-canopy friction velocity, u^*. The same result with different scaling can be obtained if the profiles are nondimensionalized with a mean wind speed being taken above the roughness layer. The friction velocity is chosen, as this velocity is a more appropriate scale for most turbulent exchange processes near the Earth's surface (Tennekes, 1982).

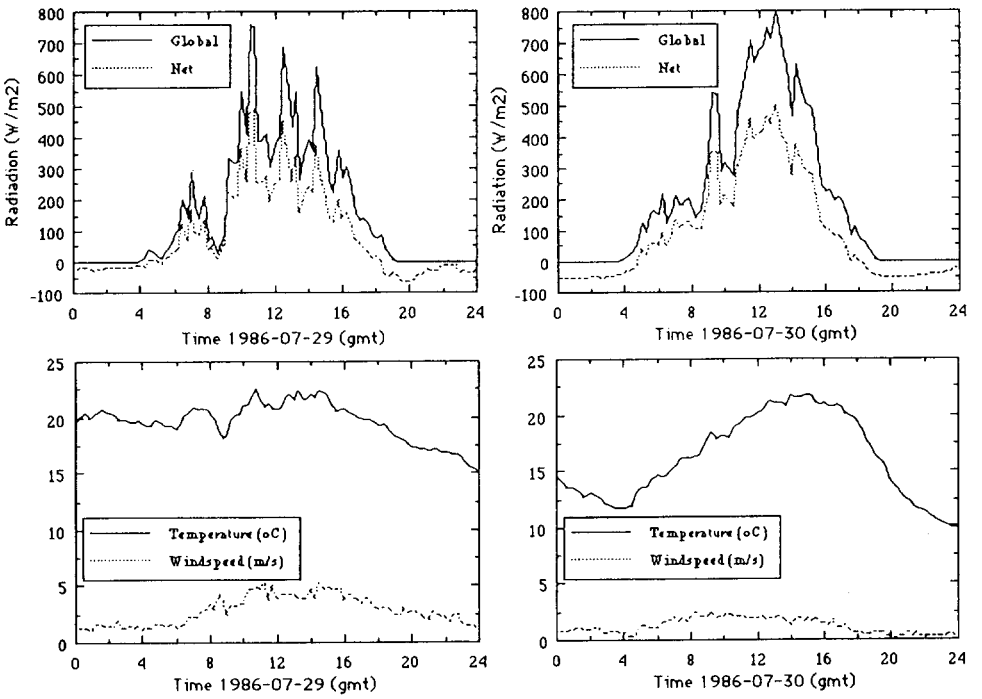

Fig. 2. General meteorological characteristics during two selected days. Temperature and wind speed are measured about 2 m above crop height.

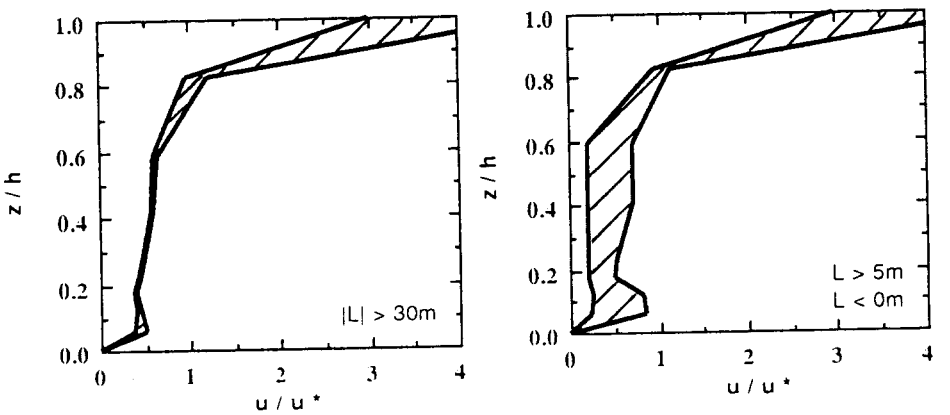

Fig. 3. The envelope containing the nondimensionalized wind profiles within the corn canopy under various thermal stratifications: left-hand part, near-neutral stratification; right-hand part, all stratifications except above-crop very stable states. The friction velocity u^* was in the range 0.4 m $s^{-1} > u^* > 0$ m s^{-1}.

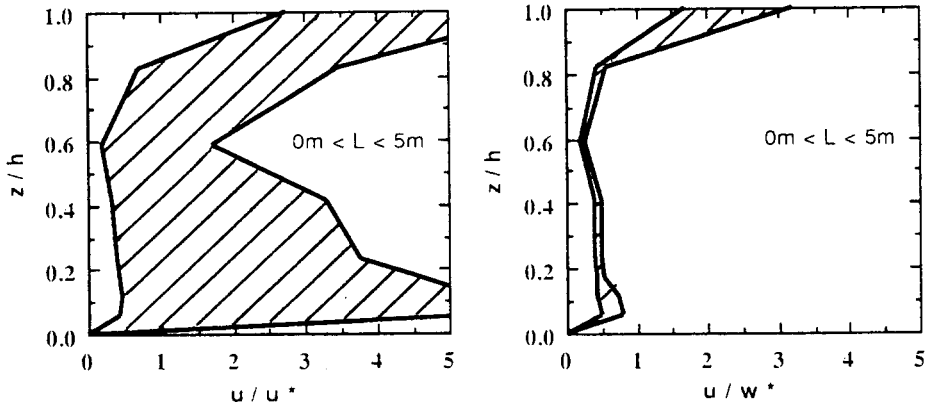

Fig. 4. The envelope of within-canopy wind speed profiles under extreme above-canopy stable conditions (0 m $< L <$ 5 m): left-hand part, nondimensionalized with the above-canopy friction velocity, u^*; right-hand part, nondimensionalized with the within-canopy free convection velocity scale, w^*.The above-canopy friction velocity was in the range 0.15 m $s^{-1} > u^* > 0$ m s^{-1}, and the within-canopy free convection scale was in the range 0.1 m $s^{-1} > w^* > 0$ m s^{-1}.

In the right-hand part of Fig. 3, in the hatched area the data fit for a wider thermal stratification range ($L > 5$ m and $L < 0$ m). From this result we can conclude not only that the thermal stratification effect and the within-canopy wind profile but also the above-canopy friction velocity, u^*, remains a suitable scaling parameter.

In the left-hand part of Fig. 4, the hatched area indicates mean wind speed profiles selected for very stable conditions above the canopy (0 m $< L <$ 5 m). This situation arose on a calm night (30 June 1986), when the top of the canopy cooled by long-wave radiative losses whereas at the soil surface the air was warmed by the soil heat flux. Under these conditions, the within-canopy air is statically unstable and decoupled from the above-canopy region. Within the canopy, and in particular in the lower region of the canopy, a free convection state occurs in which free convection cells are generated by the relatively warm soil surface. This figure shows that the envelope is extremely wide under very stable conditions, which suggests that the above-canopy friction velocity, u^*, is not relevant to within-canopy processes under very stable conditions (0 m $< L <$ 5 m).

In the right-hand part of Fig. 4, the same results have been nondimensionalized with the free convection scale, w^*. It can be inferred that, under very stable stratification above the canopy, the within-canopy free convection scaling velocity, w^*, is indeed a much better scaling parameter than the above-canopy friction velocity scale, u^*.

Fig. 4 also reveals that the absolute wind speed profiles under very stable conditions above the crop show a clear minimum at a height of $z/h = 0.6$; below $z/h = 0.6$ the free convection states dominates, whereas above this height, the wind speed forcing from above the canopy dominates. It is interesting to note that the height $z/h = 0.6$ coincides (see Fig. 1) with the maximum of the plant area distribution.

In Fig. 5 the hatched area has been plotted between which the daytime profiles of

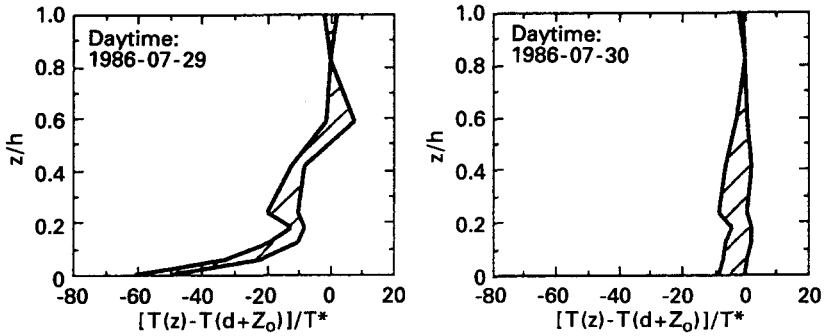

Fig. 5. The envelope of the within-canopy air temperature measured at $0.25D$ (D is row distance). The left-hand part shows daytime results of 29 July 1986, a day when the cloudiness was intermittent. The profiles are nondimensionalized with the scaling temperature T^*. The right-hand part shows the profiles measured on 30 July, a moderately fine day.

the dimensionless temperature difference, $[T(z) - T(d + z_0)]/T^*$, occur. Here, the daytime temperature profiles are nondimensionalized with the scaling temperature, T^*. The procedure has been executed in the same way as follows from general theory for the above-canopy state (see Eq. (2)). In the present study, the displacement height and roughness length have been assumed to be $d = 0.75h$ and $z_0 = 0.25(h - d)$, respectively (Jacobs and Van Boxel, 1988a,b). This means that the height $d + z_0$ agrees well with an inside canopy level of $z = 1.4$ m. This is why the mean temperature at this level has been assumed to be the reference temperature $T(d + z_0)$. Hence, the dimensionless profiles for a particular day are similar in shape under above-canopy unstable stratification, and scale well for a particular day with the above-canopy scaling temperature, T^*.

From the daytime results of Fig. 5, the shape of the dimensionless temperature profiles differs considerably for different days. Probably other processes, not included

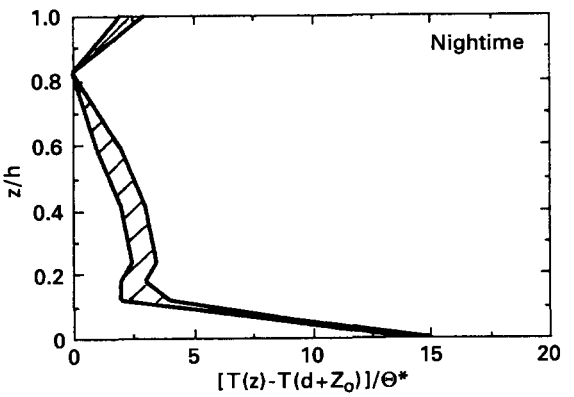

Fig. 6. The envelope of the within-canopy night-time temperature profiles under low wind speed conditions nondimensionalized with the free convective temperature scale Θ^*.

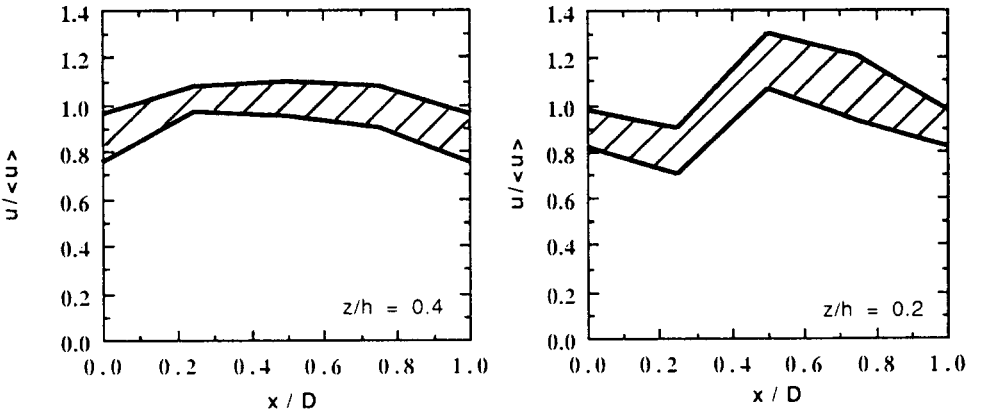

Fig. 7. The relative within-canopy mean wind speed variation at two levels ($z/h = 0.2$ and 0.4) with regard to the spatial averaged values, $\langle u \rangle$, at the same levels. All stratifications are included except above-canopy very stable states (0 m $< L <$ 5 m).

in the present temperature scale, T^*, are responsible for these effects. Two important differences between the days analysed are the irradiation regime and the wind regime (see Fig. 2). It is therefore reasonable to assume that different irradiation (i.e. differences in ratio of direct and diffusive radiation) and wind regimes will affect the shape of the temperature profiles. This also must lead to the conclusion that there is no unique simple temperature scale for daytime situations that provides a universal within-canopy temperature profile.

In Fig. 6, the results for July 1986 have been plotted for calm night-time situations when the above-canopy stratification was stable (5 m $> L >$ 0 m) and the wind speed was low ($U(10\text{m}) < 2$ m s^{-1}). Here, the profiles of the temperature difference, $T(z) - T(d + z_0)$, have been nondimensionalized with the free convection temperature scale Θ^*. It can be inferred from this result that the dimensionless profiles for both nights are similar in shape under above-canopy stable stratification and scale well with the within-canopy free convection temperature scale, Θ^*.

5. Horizontal within-canopy wind speed and temperature distribution

Fig. 7 shows the area (for levels $z/h = 0.2$ and 0.4) of the horizontal wind speed distributions relative to the spatially averaged wind speed, $\langle u \rangle$. Within a row canopy, the mean wind speed varies between 20% (top region) and 30% (lower region) from its spatially mean value. Moreover, this result suggests that in the lower region ($z/h = 0.2$) the spatial maximum occurs approximately in the centre of the row. This is expected, as in the lower region (see Fig. 1) the canopy is most sparse; in addition, the plant elements are concentrated near the stems. In the higher region ($z/h = 0.4$) the horizontal wind speed distribution is more evenly distributed. This also is expected, as in the upper region of the corn canopy the largest contribution to

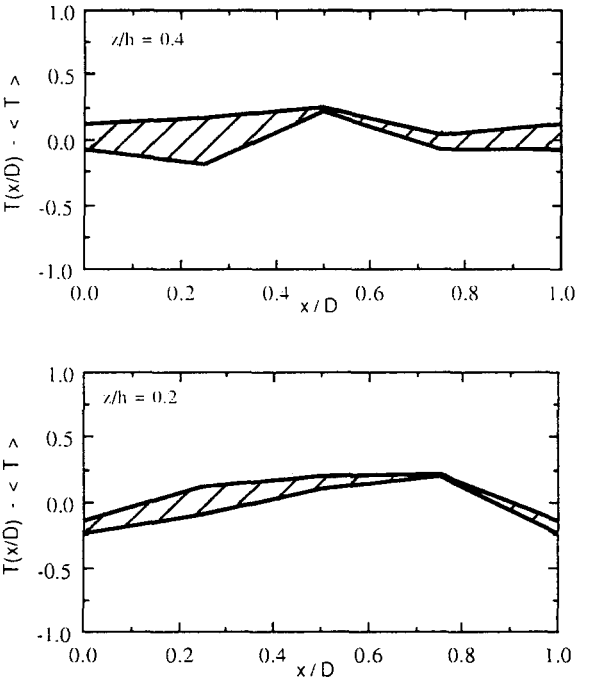

Fig. 8. The envelope of the within-canopy deviation of the within-canopy mean temperature (°C) with respect to the spatially averaged values at two levels. Top: $z/h = 0.4$; bottom: $z/h = 0.2$.

the plant area index, PAI, occurs, and in addition, the plant elements are more evenly distributed spatially.

In Fig. 8, the hatched area of the horizontal mean temperature distribution with regard to the spatially averaged temperature, $\langle T \rangle$, has been plotted for two levels ($z/h = 0.4$ and 0.2). For both levels, the maximum temperature lies more or less in the centre of the row and the minimum lies near the stems of the plants. Moreover, for both levels, with some exceptions, a mean maximum temperature difference can occur somewhere between 0.2–0.5°C, which is rather moderate. This result agrees roughly with that found by Graser et al. (1987) for their narrow-row canopy. They also found the maximum temperature in the centre of the row, but their spatial variation of about 1°C was larger than that reported here.

A few exceptions, not indicated in Fig. 8, were found around noon on the sunny day only (30 July 1986). In Fig. 9, these extremes have been portrayed in more detail, and a time course in the pattern of the horizontal temperature distribution can be observed clearly. This pattern is a result of the direct irradiation regime in conjunction with the orientation of the rows (NNE–SWW). In Fig. 9, $x/D = 1$ aligns with the western side of the row whereas $x/D = 0$ aligns with the eastern side. The influence of midday solar irradiance diminishes with depth inside the canopy.

During night-time, the above-crop wind speed drops, with a resulting decrease in the friction velocity, u^*, whereas the within-canopy free convection velocity, w^*, will

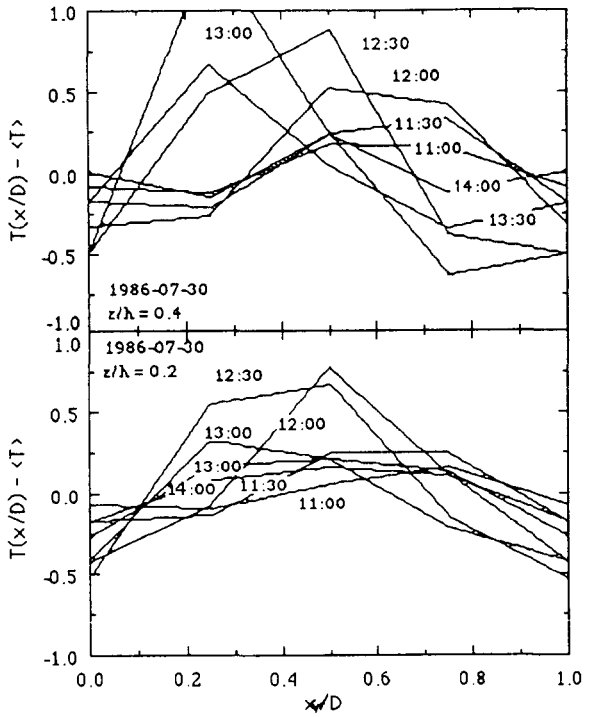

Fig. 9. The course of the horizontal variability around noon during a day when the direct irradiation dominates.

be of increasing importance. Jacobs et al. (1992) found that within the above-canopy thermal stability range of 0 m $< L <$ 5 m, the within-canopy wind speed profile scales excellently with the free convective velocity scale. Fig. 10 shows that this situation applies to periods when the convective velocity scale, w^*, exceeds the friction velocity scale, u^*.

It is of interest to find out if, when the free convective scale, w^*, dominates, the within-canopy state agrees with the following often-used criteria based on the Grashof and Reynolds numbers in technical problems (Monteith and Unsworth, 1990):

free convection: $\mathrm{Gr} > 16\mathrm{Re}^2$
forced convection: $\mathrm{Gr} < 0.1\mathrm{Re}^2$
mixed convection: $16\mathrm{Re}^2 < \mathrm{Gr} < 0.1\mathrm{Re}^2$

Here, the Grashof number is $\mathrm{Gr} = (g/T)\Delta T h^{*3}/\nu^2$ (g is gravity, h^* is characteristic length scale and v is kinematic viscosity) and the Reynolds number is $\mathrm{Re} = u^* h^*/\nu$. The length scale $h^* = d + z_0$ was chosen. In Fig. 11 these criteria as well as the results for the selected nights of 29 and 30 July have been plotted. From these, it can be observed that, when the convective velocity scale exceeds the friction velocity, the above criteria (Eqs. (4)) indicate a free convection state within the canopy. Moreover,

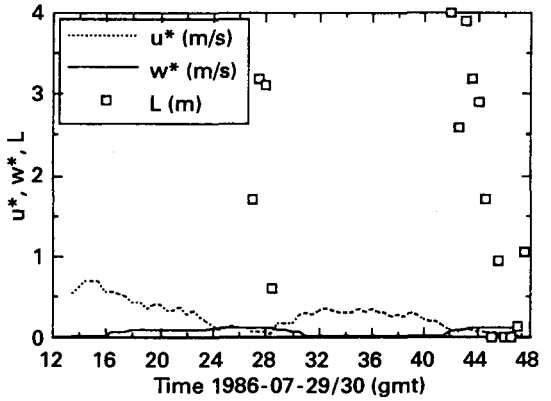

Fig. 10. The course of the friction velocity, u^*, and free convection velocity scale, w^*, during both selected days. The stability length scale, L, has been plotted only when the free convection velocity scale dominates.

during all other night-time situations, these criteria indicate a mixed convection state. However, under strong wind conditions at night the forced convection state can be reached easily.

6. Conclusions

From the foregoing results, the following main conclusions can be drawn:

(1) the horizontal variability of the mean wind speed in a row crop is restricted to about 20% of its spatial mean value. In the lower region ($z/h < 0.6$), the maximal value occurs in the centre between the rows and the minimal value occurs

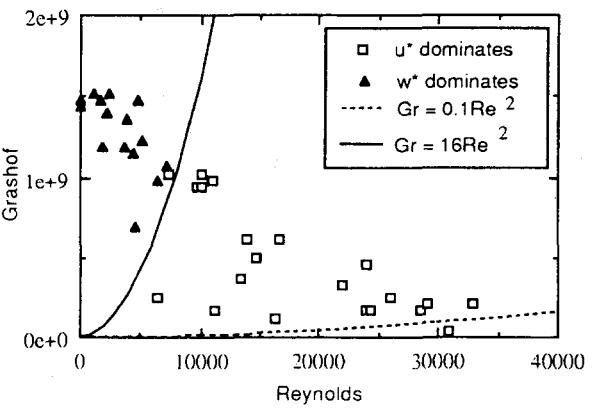

Fig. 11. The Grashof number ($\mathrm{Gr} = (g/T)h^{*3}\Delta T/\nu^2$, where $h^* = d + z_0$) vs. the Reynolds number ($\mathrm{Re} = u^*h^*/\nu$). For night-time observations, the free convection criterion, $\mathrm{Gr} = 16\mathrm{Re}^2$, and the forced convection criterion, $\mathrm{Gr} = 0.1\mathrm{Re}^2$), have been indicated.

near the stems. In the upper region ($z/h > 0.6$), the horizontal distribution is more even.

(2) In most stratification states ($L > 5$ m and $L < 0$ m) the within-canopy mean wind profiles can be scaled satisfactorily by the above-canopy friction velocity, u^*, or by a mean above-canopy reference wind speed. This means that above-canopy and within-canopy flow is strongly coupled.

(3) Under very stable stratification above the canopy ($0\text{ m} < L < 5\text{ m}$) a decoupling between the above-canopy and within-canopy flow occurs. Here, the within-canopy free convective flow is forced mainly by the soil heat flux. The height of the convective cells is restricted by the top layer of the canopy, where long-wave radiative losses cause a strong thermal temperature inversion. The height of the free convection region coincides with the maximum of the plant density distribution.

(4) In a moderate climate the maximum horizontal variability within the mean temperature profile of a dense homogeneous row canopy lies somewhere around 2°C during the day and around 4°C at night.

(5) The horizontal variability of the mean air temperature in a row crop is moderate and restricted to about 0.35°C of its spatial mean value. The maximum value occurs in the centre between the rows and the minimum value occurs near the stems. The same pattern is observed in the upper as well as the lower canopy region. Exceptions occur around midday, when direct radiation dominates. Then, a variation of 1°C or more can be observed.

(6) During unstable stratification states (daytime) the within-canopy mean temperature profiles can be scaled well by the above-canopy scaling temperature, T^*, for a particular irradiation and wind speed regime. This means that, under these conditions, above-canopy and within-canopy flow is strongly coupled.

(7) During nights with low wind, a decoupling between the above-canopy and within-canopy flow occurs. The within-canopy free convective flow is forced by the soil heat flux at the floor of the canopy. Under these conditions, the within-canopy temperature profiles scale well with the free convective within-canopy temperature scale, Θ^*.

(8) The criteria of Eqs. (4) apply well for the within-canopy heat transport process to distinguish the convection type. The boundary between the free convection and mixed convection states can also be found by comparing the above-canopy friction velocity and the within-canopy free convective velocity scale.

(9) In modelling transport processes within a plant canopy, the present results suggest that during the day mixed convection nearly always dominates, whereas during the night, when w^* is greater than u^*, the free convection dominates.

Acknowledgements

The authors' grateful thanks are offered to the Institute for Land and Water Management (ICW) for permission to use facilities of the experimental farm at Sinderhoeve. J.H. van Boxel was supported financially by the Working Group on

Meteorology and Physical Oceanography (MFO) of the Netherlands Organization for Advancement of Pure Physics (ZWO). R.M.M. El-Kilani was financially supported by WOTRO.

References

Arya, S.P., 1988. Introduction to Micrometeorology. Academic Press, San Diego, CA, 307 pp.

Finnigan, J.J. and Raupach, M.R., 1987. Transfer processes in plant canopies in relation to stomatal characteristics. In: E. Zeiger (Editor), Stomatal Function. Stanford University Press, Stanford, CA, pp. 385–429.

Garratt, J.R. and Segal, M., 1988. On the contribution to dew formation. Boundary-Layer Meteorol., 45: 209–236.

Graser, E.A., Verma, S.B. and Rosenberg, N.J., 1987. Within-canopy temperature patterns of sorghum at two row spacings. Agric. For. Meteorol., 41: 187–205.

Jacobs, A.F.G. and van Boxel, J.H., 1988a. Changes of the displacement height and roughness length of maize during a growing season. Agric. For. Meteorol., 42: 53–62.

Jacobs, A.F.G. and van Boxel, J.H., 1988b. Computational parameter estimation for a maize crop. Boundary-Layer Meteorol., 42: 265–279.

Jacobs, A.F.G., van Boxel, J.H. and Shaw, R.H., 1992. The dependence of canopy layer turbulence on within-canopy thermal stratification. Agric. For. Meteorol., 58: 247–256.

Kvet, J. and Marshall, J.K., 1971. Assessment of leaf area and other assimilating plant surfaces. In: Z. Sastak, J. Catsky and P.G. Jarvis (Editors), Plant Photosynthesis Production: Manual of Methods. Dr. W. Junk, The Hague, pp. 517–574.

Monteith, J.L. and Unsworth, M.H., 1990. Principles of Environmental Physics. Edward Arnold, London, 291 pp.

Mulhearn, P.J. and Finnigan, J.J., 1978. Turbulent flow over a very rough, random surface. Boundary-Layer Meteorol., 15: 109–132.

Shaw, R.H., den Hartog, G., King, K.M. and Thurtell, G.W., 1974. Measurements of mean wind flow and three dimensional turbulence intensity within a mature corn canopy. Agric. Meteorol., 13: 419–425.

Stigter, C.J., Birnie, J. and Jansen, P., 1976. Multi-point temperature measuring equipment for crop environment, with some results on horizontal homogeneity in a maize crop. Neth. J. Agric. Sci., 24: 223–237.

Tennekes, H., 1982. Similarity relations, scaling and spectral dynamics. In: F.T.M. Nieuwstad and H. van Dop (Editors), Atmospheric Turbulence and Air Pollution Modeling. D. Reidel, Dordrecht, pp. 37–68.

Tennekes, H. and Lumley, J.L., 1972. A First Course in Turbulence. MIT Press, Cambridge, MA, 300 pp.

Van Asselt, C.J., Jacobs, A.F.G., van Boxel, J.H. and Jansen, A.E., 1991. A rigid fast-response thermometer for atmospheric research. Meas. Sci. Technol., 2: 26–31.